Available online at www.sciencedirect.com
ScienceDirect
Geochimica et Cosmochimica Acta 70 (2006) 5831–5841
Geochimica
www.elsevier.com/locate/gca

Effect of hydrogen limitation and temperature on the fractionation of sulfur isotopes by a deep-sea hydrothermal vent sulfate-reducing bacterium

Joost Hoek [a,b,c,*], Anna-Louise Reysenbach [b], Kirsten S. Habicht [c], Donald E. Canfield [c]

[a] *Department of Earth and Environmental Science, University of Pennsylvania, Philadelphia, PA 19104, USA*
[b] *Department of Biology, Portland State University, Portland, OR 97201, USA*
[c] *Nordic Center for Earth Evolution (NordCEE) and Institute of Biology, University of Southern Denmark, Odense, Denmark*

Received 31 May 2005; accepted in revised form 26 July 2006

Abstract

The fractionation of sulfur isotopes by the thermophilic chemolithoautotrophic *Thermodesulfatator indicus* was explored during sulfate reduction under excess and reduced hydrogen supply, and the full temperature range of growth (40–80 °C). Fractionation of sulfur isotopes measured under reduced H_2 conditions in a fed-batch culture revealed high fractionations (24–37‰) compared to fractionations produced under excess H_2 supply (1–6‰). Higher fractionations correlated with lower sulfate reduction rates. Such high fractionations have never been reported for growth on H_2. For temperature-dependant fractionation experiments cell-specific rates of sulfate reduction increased with increasing temperatures to 70 °C after which sulfate-reduction rates rapidly decreased. Fractionations were relatively high at 40 °C and decreased with increasing temperature from 40–60 °C. Above 60 °C, fractionation trends switched and increased again with increasing temperatures. These temperature-dependant fractionation trends have not previously been reported for growth on H_2 and are not predicted by a generally accepted fractionation model for sulfate reduction, where fractionations are controlled as a function of temperature, by the balance of the exchange of sulfate across the cell membrane, and enzymatic reduction rates of sulfate. Our results are reproduced with a model where fractionation is controlled by differences in the temperature response of enzyme reaction rates and the exchange of sulfate in and out of the cell.
© 2006 Elsevier Inc. All rights reserved.

1. Introduction

The sequential reduction of sulfate to sulfide during dissimilatory sulfate reduction leads to a fractionation of sulfur isotopes. The fractionation of ^{34}S during dissimilatory sulfate reduction by pure cultures has been extensively studied, especially for mesophilic *Desulfovibrio* species (e.g., Thode et al., 1951; Harrison and Thode, 1958; Kaplan and Rittenberg, 1964; Kemp and Thode, 1968; Smejkal et al., 1971; Chambers et al., 1975; McCready, 1975; Bottcher et al., 1999; Bolliger et al., 2001; Detmers et al., 2001; Habicht et al., 2005; Johnston et al., 2005; Canfield et al., 2006). Results from these pure-culture studies show wide ranging fractionations of ^{34}S from 3‰ to 46‰ with an average around 18‰ (Canfield and Teske, 1996). While some of this variability results from inherent differences between organisms (Bolliger et al., 2001; Detmers et al., 2001; Kleikemper et al., 2004), environmental variables such as electron donor type and concentration, sulfate concentration, and temperature have also been shown to control the extent to which individual species of sulfate-reducing microorganisms fractionate sulfur isotopes (Harrison and Thode, 1958; Kaplan and Rittenberg, 1964; Kemp and Thode, 1968; Chambers et al., 1975; Habicht et al., 2005; Canfield et al., 2006).

Research documenting the effect of different environmental variables on fractionation has shown that for indi-

* Corresponding author.
E-mail address: joost@biology.sdu.dk (J. Hoek).

0016-7037/$ - see front matter © 2006 Elsevier Inc. All rights reserved.
doi:10.1016/j.gca.2006.07.031

vidual species of sulfate-reducing microorganisms the extent of fractionation is dependent on cell specific rates of sulfate reduction (expressed in mol cell^{-1} time^{-1}) (Harrison and Thode, 1958; Kaplan and Rittenberg, 1964; Kemp and Thode, 1968; Chambers et al., 1975; Canfield et al., 2006). In many cases, when an organic electron donor is supplied fractionation decreases with increasing sulfate reduction rates. Increasing sulfate reduction rates linked to decreasing fractionations have been associated with increasing temperatures and increasing supplies of organic electron donors. Conversely, when H_2 is the electron donor fractionations have been shown to increase with increasing sulfate reduction rates (Kaplan and Rittenberg, 1964). Fractionations have also been observed to be suppressed under a number of circumstances, including low sulfate concentrations (below ~200 μM) (Harrison and Thode, 1958; Habicht et al., 2002), when H_2 is used as the electron donor (Kaplan and Rittenberg, 1964; Kemp and Thode, 1968), and at temperatures approaching the minimum for growth of individual species (Kaplan and Rittenberg, 1964; Kemp and Thode, 1968). The patterns on the control of fractionation summarized above are not always observed. For example, in gradient temperature experiments similar to the ones performed here, Canfield et al. (2006) observed a positive trend between sulfate reduction rates and fractionation, with higher fractionations observed at lower temperatures. These 'nonstandard' results were explained with a fractionation model based on the network of Rees (1973), where the extent of fractionation depended on a balance between the temperature dependence of the exchange rate of sulfate in and out of the cell and the exchange of the internal sulfur pools.

Only limited work has been done to measure fractionation during sulfate reduction with H_2 as electron donor. Nevertheless, these results have shown that when H_2 is used during sulfate reduction, fractionations are significantly reduced when compared to fractionations produced during sulfate reduction with organic compounds. As an example, in the classic study of Kaplan and Rittenberg (1964) sulfate reduction with H_2 produced fractionations in the range of 5–10‰ under similar growth conditions where sulfate reduction with organic compounds produced fractionations in the 25–35‰ range. The reasons for reduced fractionations with H_2 are unclear, but Kaplan and Rittenberg (1964) suggest that with H_2, the reduction of sulfate to sulfite (through APS) is rate limiting, allowing only limited expression of the fractionation during subsequent enzymatic reductions downstream from this step. It is important to note however, that most experiments with H_2 as electron donor have been conducted in batch culture with H_2-saturated head-space. It is unlikely that these conditions provide the same substrate limitation as might occur in nature. Part of our experimental approach was to conduct fractionation experiments where H_2 supply was limited during sulfate reduction. A second approach was to conduct fractionation experiments where temperature was the controlling environmental variable. In this way we can constrain how temperature influences fractionation, and because temperature controls enzyme reaction rates and sulfate reduction rates, we could systematically explore how changes of these variables influenced fractionation. Our overall goal was to establish a stronger understanding for how growth with H_2 controls fractionation during sulfate reduction. This is significant because H_2 is likely to be an important substrate to drive sulfate reduction in nature (see review in Canfield et al., 2005).

We conducted our experiments using *Thermodesulfotator indicus*, strain CIR29812, a thermophilic chemolithoautotroph recently isolated from a deep-sea hydrothermal vent on the Central Indian Ridge (Moussard et al., 2004). This organism may be important in sulfate reduction in hydrothermal systems, and because it is the deepest-branching sulfate reducing bacteria isolated to date, according to 16S rDNA phylogenetics (Moussard et al., 2004), it may improve our understanding of sulfur isotope fractionations preserved in the geologic record.

2. Materials and methods

2.1. Culture conditions

Thermodesulfotator indicus was maintained in anaerobic salt-water carbonate buffered medium with H_2 as the electron donor and CO_2 as the primary carbon source. The medium contained per liter of H_2O, 20 g NaCl, 3 g $MgCl{\cdot}6H_2O$, 0.15 g $CaCl_2{\cdot}2H_2O$, 4.0 g Na_2SO_4 (final concentration of sulfate = 28 mM), 0.25 g NH_4Cl, 0.2 g KH_2PO_4, 0.5 g KCl, 1 ml of trace element mixture (Moussard et al., 2004), 1 ml of vitamin solution (Moussard et al., 2004), 1 ml of 10% yeast extract, and 1 ml of 2 M Na-acetate solution. Yeast extract and acetate were added as a growth stimulant and are not used by *T. indicus* as an energy source (Moussard et al., 2004). The medium was prepared anaerobically and 50 ml was aseptically transferred into sterile anaerobic 100-ml serum bottles sealed with black butyl rubber stoppers. The headspace was flushed with a H_2/CO_2 mixture (80:20 v/v) and subsequently pressurized to 2 atm. The pH of the medium was adjusted to 6.25 with 5 N HCl. Fifty milliliters stock cultures were grown at 70 °C. To ensure reproducible growth conditions, cultures were transferred twice into fresh media prior to the start of each experiment.

2.2. H_2-dependent fractionation experiments

Hydrogen-dependant growth experiments were performed in a 1.2-L bioreactor with a 1-L working volume. A summary of the bioreactor set-up and control is provided below, however, a more detailed description has been reported elsewhere (Hoek et al., 2006). All experiments were carried out at 70 °C, pH 6.25, under fed-batch culture. This is a type of batch culture that is fed continuously with a nutrient medium (e.g., H_2). Medium for the growth experiments in the bioreactor was prepared as described

above, except that a CO_2/N_2 mixture (80:20 v/v) and H_2 were continuously sparged into the bioreactor. The volumetric flow rate of CO_2/N_2 through the reactor was held constant at 200 ml min^{-1} for all experiments. The volumetric flow rate of H_2 into the reactor was changed for different experiments (Table 1). Two non-substrate limiting experiments were run where excess H_2 was supplied to the culture media at a flow rate of 10 ml min^{-1}. Although the concentration of H_2 was not monitored in the bioreactor, increasing flow rates of H_2 beyond 10 ml min^{-1} did not increase specific growth rates above the measured maximum growth rates (with H_2 flow rates of 10 ml min^{-1}) indicating that hydrogen availability was not limiting sulfate reduction rates in these experiments. Using Henry's law and correcting for salinity (ionic strength = 0.7) and temperature (70 °C), we calculated maximum H_2 concentrations in the high-flux experiments to be ~34 μM. Two subsequent experiments were run where H_2 supply was reduced to 2 and 1.5 ml min^{-1}.

In all bioreactor experiments, gas-flow rates were regularly calibrated using an ADM 1000 flow meter (Agilent, USA). The effluent gas, containing a mixture of N_2, CO_2, H_2, and biogenic H_2S, was passed through a condenser at 4 °C to reduce evaporation from the culture medium, and subsequently sparged through a sulfide trap containing 2 L of 5% $ZnCl_2$ under anaerobic conditions. Sulfide reacts with $ZnCl_2$ to form $ZnS_{(solid)}$ and HCl. The pH of the sulfide trap was held constant by base titration. To ensure that there was no loss of H_2S from the system, the effluent gas from the first trap was transferred to a second sulfide trap. This trap was visually monitored for ZnS precipitation, although no precipitation was observed in any of the experiments. The concentration of sulfide in the bioreactor was monitored at regular intervals during the course of each experiment and indicated that no appreciable sulfide remained in the bioreactor. The sulfide traps were changed between experiments. Prior to the start of each experiment, the reactor was brought to equilibrium by sparging with CO_2/N_2 (80:20 v/v) and H_2 at 70 °C overnight.

Continuous online estimation of growth parameters was accomplished by computer-controlled base titration in the sulfide trap to maintain constant pH (Hoek et al., 2006). During the course of each experiment, growth was monitored by measuring the optical density (OD, $\lambda = 595$ nm) of the culture and by sulfate and sulfide analysis of sample aliquots taken at regular intervals from the bioreactor and sulfide trap. Samples were immediately frozen after collection and stored for sulfate and sulfide analysis (see Section 2.5).

Table 1
Isotope fractionation during sulfate reduction by fed-batch cultures of *T. indicus* with H_2 supplied as limiting and non-limiting substrate

Experiment No.	H_2 flow rate (ml min^{-1})	Specific growth rate (h^{-1})	ssSRR (fmol SO_4 $cell^{-1}$ h^{-1})	ε (‰)
High H_2-flux experiments				
1	10	0.30	18–20	1.5–6.4
2	10	0.36	22–23	4.4–5.5
Low H_2-flux experiments				
3	2	0.009	3–5	28.2–35.9
4	1.5	0.008	2–3	24.5–37.9

2.3. Temperature-dependent fractionation experiments

Temperature dependant fractionation of sulfur isotopes during sulfate reduction was studied using a thermal-gradient block (Elsgaard et al., 1994). A stable temperature gradient was established in an insulated aluminum block of 1m length, cooled to 35 °C at one end and heated to 80 °C at the other. This temperature range was chosen to cover the full range of growth temperatures for *T. indicus* (40–80 °C). Two parallel slots for each of 16 equidistant incubation temperatures were used during the growth experiments. The temperature gradient in the block was checked at regular intervals and remained constant within ±0.6 °C.

Medium for temperature-dependent growth experiments was prepared as described above. Growth experiments were performed in 15-ml Hungate tubes. The headspace in the sample tubes was flushed with CO_2/N_2 (80:20 v/v), and tubes were sealed with black butyl rubber stoppers and capped. Sterile anaerobic media was prepared prior to the start of each experiment, and 5 ml was aseptically transferred to each Hungate tube prior to inoculation. One half ml of stock culture was aseptically transferred to each tube immediately preceding the start of each experiment, and each tube was then flushed with a H_2/CO_2 mixture (80:20 v/v) and pressurized to 2 atm. Under these conditions, H_2 is supplied as a 'non-limiting' energy source, as indicated by a period of exponential growth of batch cultures at optimized growth temperatures (70 °C). Tubes were incubated at different temperatures along the length of the heat block.

Growth was followed by measuring the OD ($\lambda =$ 595 nm) of the culture in each tube. Cultures which had grown to mid- or late-exponential phase were injected with 0.2 ml of 20% ZnAc. This precipitated all sulfide as ZnS, and stopped growth. Samples were immediately frozen and stored for sulfate and sulfide analysis (see Section 2.5).

2.4. Cell-specific sulfate reduction rates

Optical density measurements were calibrated to cell growth by performing cell counts on cultures across a range of OD values. Cell counting was performed using an Axioplan phase-contrast microscope (Carl Zeiss, Jena, Germany). Prior to counting, cells were fixed in 4% glutaraldehyde and stained with 4′,6′-diamidino-2-phenylindole (DAPI) (Porter and Feig, 1980). Cell-specific sulfate reduction rates (csSRR, in fmoles $cell^{-1}$ h^{-1}) were calculated for the exponential phase using the change in concentration of

sulfate and cell number (cn) between two selected time points (t_1 and t_2) according to the following equation (Detmers et al., 2001):

$$\mathrm{csSRR} = \frac{\left[SO_4^{2-}{}_{(2)}\right] - \left[SO_4^{2-}{}_{(1)}\right]}{\frac{[cn_{(1)}+cn_{(2)}]}{2}(t_2 - t_1)}. \quad (1)$$

2.5. Analytical methods

The sulfate concentration was measured by suppressed-ion chromatography, using a Sykam LAC A14 column (3 × 250 mm, 70 °C). Five millimolars $NaCO_3$ with 1% hydroxybenzonitrile (v/v) was used as effluent. The effluent flow rate was 1.5 ml/min. The concentration of sulfide (±5%) was determined spectrophotometrically at 670 nm on ZnS-preserved samples with the methylene-blue technique (Cline, 1969).

For isotope analysis, ZnS was acid distilled with 6N HCl into a silver nitrate solution, precipitating Ag_2S. The sulfate for isotope analysis was precipitated with 1 M $BaCl_2$ as $BaSO_4$. Precipitated samples were dried, and 300–400 μg of sample was weighed into tin cups with a 10-fold excess of vanadium pentoxide (V_2O_5). Samples were converted to SO_2 during combustion with oxygen at 1080 °C. The SO_2 gas was purified by gas chromatography. Isotope analysis was undertaken using elemental-analyzer combustion-flow isotope-ratio mass spectrometry (IRMS) (Giesemann et al., 1994).

The reference material used in the analysis of the capsules was NBS-127 (barium sulfate, $\delta^{34}S_{V\text{-}CDT} = +20.3‰$) distributed by the International Atomic Energy Association (IAEA). NBS-127, IAEA-S-1 (silver sulfide, $\delta^{34}S_{V\text{-}CDT} = -0.30‰$), and Iso-Analytical R-025 (barium sulfate, $\delta^{34}S_{V\text{-}CDT} = +8.53‰$) were used for calibration and correction of the ^{18}O contribution to the SO^+ ion beam. NBS-127, IAEA-S-1, and IA-R-025 were also run to check analytical accuracy. All isotope values are reported as parts per thousand (‰) deviations from the Canon Diablo Troilite (CDT) standard (±0.5‰).

2.6. Fractionation calculations

In both the fed-batch culture and thermal-gradient-block experiments, the sum of the sulfide produced during sulfate reduction and the remaining sulfate at the end of each experiment clustered around the input sulfate concentration (within analytical error of ±5%), indicating a conserved system. Therefore, as sulfate is depleted during sulfate reduction, the isotopic difference between sulfate and sulfide develops according to a Rayleigh distillation model, and does not provide a direct measure of fractionation (Canfield, 2001a). As the sulfate concentration decreases, the isotopic composition of the sulfide approaches that of the original sulfate, and after the original sulfate is completely consumed, no fractionation information is preserved. In our thermal gradient block incubation experiments, the cultures reduced between 4% and 94% of the starting sulfate concentration to sulfide. Therefore, a Rayleigh distillation model was used to calculate the true fractionations. The isotopic composition of sulfate in both the fed-batch culture experiments and heat-block experiments evolves according to

$$\delta_{SO_4(out)} = (\delta_{SO_4(in)} + 1000) * f_{SO_4}^{(1-\alpha_{SR})} - 1000 \quad (2)$$

where $\delta_{SO_4(in)}$ is the isotopic composition of the original sulfate, $\delta_{SO_4(out)}$ is the composition of the output sulfate, α_{SR} is the fractionation factor imposed during sulfate reduction, and f_{SO_4} is the fraction of the input sulfate remaining. This equation can be solved for α_{SR}

$$\alpha_{SR} = 1 + [\ln(\delta_{SO_4(in)} + 1000) - \ln(\delta_{SO_4(out)} + 1000)] / \ln(f_{SO_4}) \quad (3)$$

With small depletions in sulfate it is more accurate to calculate fractionations from the output isotopic composition of sulfide rather than sulfate. These two are related by the equation

$$\delta_{SO_4(out)} = (\delta_{SO_4(in)} - f_{H_2S} * \delta_{H_2S(out)}) / f_{SO_4} \quad (4)$$

where $\delta_{H_2S(out)}$ is the isotopic composition of sulfide produced during sulfate reduction, f_{H_2S} is the fraction of original sulfate converted to sulfide during sulfate reduction, and

$$f_{SO_4} + f_{H_2S} = 1 \quad (5)$$

The fractionation during sulfate reduction is reported using the ε notation ($\varepsilon_{SR}‰$), and is given by

$$\varepsilon_{SR} = (\alpha_{SR} - 1) * 1000. \quad (6)$$

3. Results

3.1. H_2-dependent fractionation experiments

Hydrogen dependant fed-batch growth experiments were performed to measure fractionation ($\varepsilon_{SO_4-H_2S}$) under conditions of excess and reduced hydrogen supply. Taking all data together (Fig. 1), fractionation trends in these experiments were inversely dependant on the rate of sulfate reduction as predicted by many observations of the relationship between csSRR and fractionation (Thode et al., 1951; Harrison and Thode, 1958; Kaplan and Rittenberg, 1964; Kemp and Thode, 1968; Chambers et al., 1975; Canfield, 2001b). In the experiments where H_2 was supplied in excess, csSRR were high and ranged from 18 to 24 fmoles SO_4^{2-} $cell^{-1}$ h^{-1}, with maximum specific growth rate (μ) of 0.3–0.36 h^{-1} (Table 1). These are at the high end of growth rates reported for sulfate-reducers (see summary in Canfield, 2001a). Fractionations varied from 1‰ to 5‰ during exponential growth (Fig. 1). These low fractionations are typical for H_2 as the electron donor in batch cultures

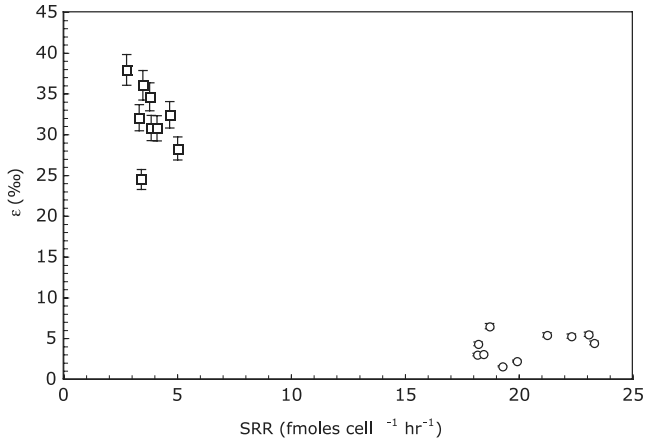

Fig. 1. Plot showing change in fractionation with cell-specific sulfate-reduction rate during fed-batch culture experiments. Squares: low-H_2-flux experiments, circles; high-H_2-flux experiments. Error bars reported as standard deviation.

(avg. <10‰, max = 19‰) (Kaplan and Rittenberg, 1964; Kemp and Thode, 1968).

In the H_2-limited experiments, specific growth rates dropped ~50-fold, to 0.008–0.009 h^{-1}, with csSRR in the range of 2–5 fmoles SO_4^{2-} $cell^{-1}$ h^{-1}. Under these conditions, fractionations increased to 24–37‰ (Fig. 1). These fractionation values are significantly higher than any fractionation values previously reported during sulfate reduction with H_2 as the electron donor, and higher than the average fractionation observed by pure cultures of sulfate-reducing prokaryotes metabolizing on organic substrate (18‰) (Canfield and Teske, 1996). Specific rates of sulfate reduction decreased slightly over the time-course of each experiment with reduced H_2 supply, which may have resulted from the progression towards increasing H_2 limitation as biomass accumulated in the bioreactor. Fractionation over the course of these experiments increased as sulfate reduction rates decreased (Fig. 1).

3.2. Temperature-dependent fractionation experiments

Two sets of thermal-gradient-block experiments were conducted to measure the fractionation of sulfur isotopes by *T. indicus* under a wide range of temperatures. Specific growth rates calculated for the exponential growth phase increased with increasing temperatures reaching maximum values (0.15 h^{-1}) around 70 °C (Fig. 2A). Specific growth rates dropped rapidly at temperatures above 70 °C. Specific rates of sulfate reduction (fmoles SO_4^{2-} $cell^{-1}$ h^{-1}), which are a measure of metabolic rate, closely followed the trends for specific growth rates, reaching the highest rates (11–12 fmoles SO_4^{2-} $cell^{-1}$ h^{-1}) around 68–70 °C (Fig. 2B). The maximum specific growth rates and csSRR for the thermal gradient block experiments were lower than the maximum rates experienced during the fed-batch experiments supplied with excess H_2 by a factor of two. This

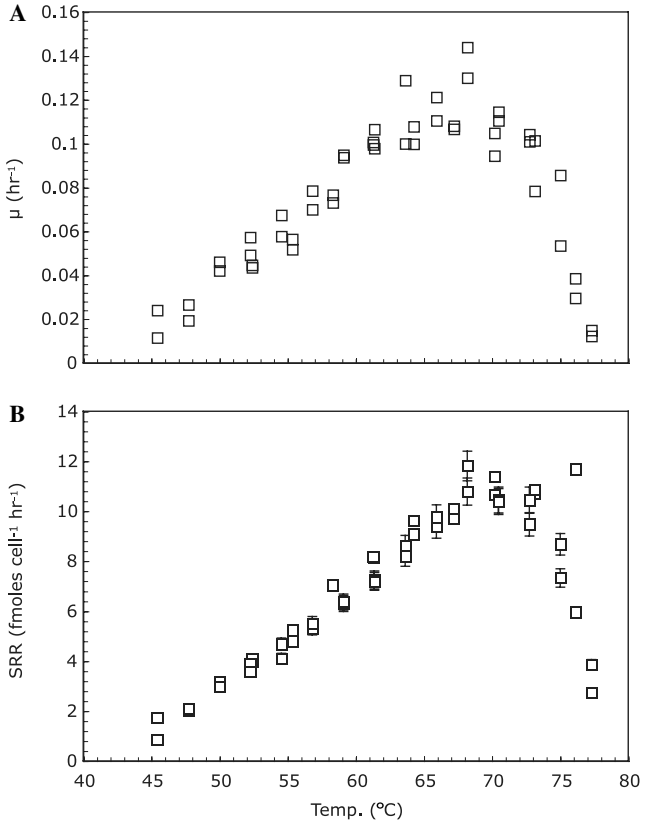

Fig. 2. Change in specific growth rate (μ) (A) and cell-specific sulfate-reduction rate (B) over the temperature range of the thermal-gradient-block experiments. Error bars reported as standard deviation.

difference may result from limited diffusion of H_2 to the media in the batch cultures of the thermal-gradient block, whereas cultures in the bioreactor were continuously sparged with H_2 and thoroughly mixed.

The fractionation is shown as a function of temperature (Fig. 3A) and specific rates of sulfate reduction (Fig. 3B). The extent of fractionation ranged from 1.1‰ to 9.7‰. These values are typical for fractionation resulting from growth with hydrogen as the electron donor (Kaplan and Rittenberg, 1964; Kemp and Thode, 1968), and are similar to the range we observed in the fed-batch experiments with non-limiting H_2. Fractionation varied systematically as a function of temperature being highest at the high and low temperatures, and the lowest in between (~60 °C). When compared to csSRR and considering temperatures below 70 °C, the highest fractionations were observed at both the highest and the lowest cell specific rates of sulfate reduction with the lowest fractionation in the intermediate range. This translates into decreasing fractionation with increasing csSRR for temperatures between 45 and 60 °C, and into increasing fractionation with increasing csSRR for temperatures between 60 and 70 °C. Above 70 °C, fractionation was more variable but generally increased with rapidly decreasing csSRR. The highest fractionation (~10‰) occurred at the highest temperature (77 °C) for which consistent growth occurred.

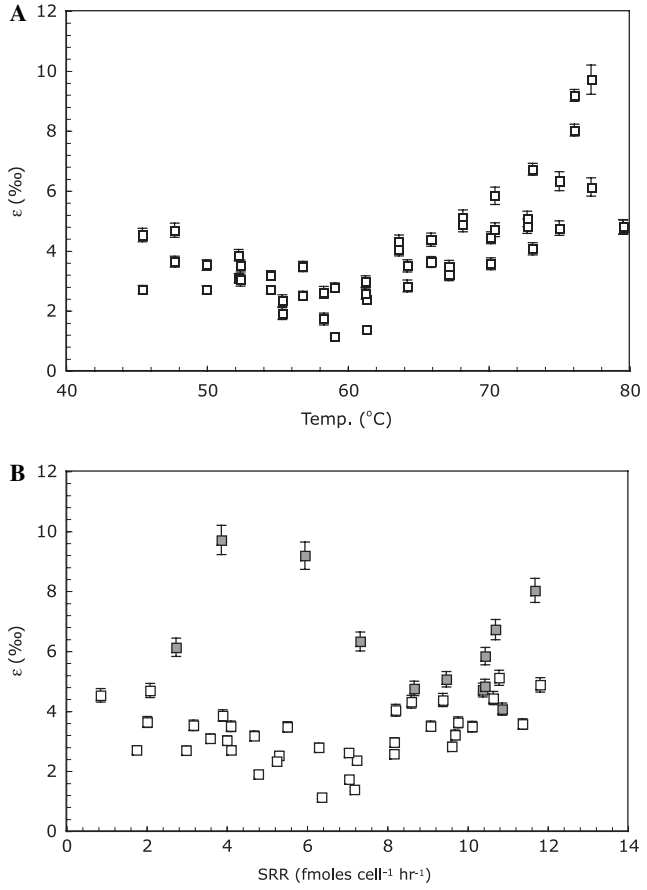

Fig. 3. (A) Change in sulfur-isotope fractionation as a function of (A) growth temperature and (B) cell-specific sulfate-reduction rate. Shaded symbols indicate experiments carried out at temperatures above 70 °C. Error bars reported as standard deviation.

4. Discussion

4.1. Factors controlling fractionation

The fractionation of sulfur isotopes during dissimilatory sulfate reduction results from a series of sequential biochemical reactions that operate at different efficiencies and with different fractionation factors. The biosynthetic pathways and associated fractionation processes of dissimilatory sulfate reduction have been extensively studied (Harrison and Thode, 1958; Peck, 1961; Kaplan and Rittenberg, 1964; Kemp and Thode, 1968; Rees, 1973). Based on the observed isotope fractionation trends, Rees (1973) developed a model that describes the principal steps in the sulfate reduction process as

$$SO_{4\,(out)}^{=} \overset{1}{\rightleftarrows} \left[SO_{4\,(in)}^{=} \overset{ATP\downarrow 2}{\leftrightarrows} APS \overset{e^-\downarrow 3}{\rightleftarrows} SO_3^{=} \right] \overset{e^-\downarrow 4}{\rightarrow} H_2S \qquad (7)$$

In this reaction network, sulfate is actively taken up by the cell together with sodium ions or protons to preserve charge balance (step 1). Sulfate transport across the cell membrane is reversible (Cypionka, 1995), allowing exchange of sulfate in and out of the cell. A small isotope fractionation of −3‰ to 0‰ ($\varepsilon_{SO_4(out)-SO_4(in)}$) is thought to be associated with this step. Once sulfate enters the cell it is activated with ATP by ATP sulfurylase to form adenosine 5′-phosphosulfate (APS) (step 2), which is reduced to sulfite (step 3) by adenylylsulfate (APS) reductase. Steps 2 and 3 are both reversible. No fractionation is expected with the activation of sulfate, but a 22–25‰ isotopic fractionation ($\varepsilon_{SO_4-SO_3}$) is assigned to APS reduction to sulfite (Harrison and Thode, 1957; Harrison and Thode, 1958). The final reduction of sulfite to hydrogen sulfide along step 4 occurs by sulfite reductase. Although sulfite reductase enzymes catalyze the oxidation of sulfide to sulfite in oxidative metabolisms (Dahl and Trüper, 1994), the reversibility of sulfite reduction (step 4) has never been demonstrated (Canfield, 2001a). A 25‰ isotope fractionation ($\varepsilon_{SO_3-H_2S}$) is normally ascribed to this step (Kemp and Thode, 1968; Rees, 1973). Brunner and Bernasconi (2005) recently proposed an alternative to the 'Rees network' summarized above. Their model differs from that developed by Rees (1973) in that it includes a multi-step reduction of sulfite, and assumes that sulfite reduction is a reversible process. Additionally, they propose much larger fractionation factors ($\varepsilon_{SO_3-H_2S} = 58‰$) during the sulfite reduction step. The implications of this model are that maximum fractionations >70‰ are possible during dissimilatory sulfate reduction.

4.2. Isotope fractionation

As summarized in the introduction, the extent of fractionation during sulfate reduction is controlled by environmental factors, such as temperature and substrate concentrations, that influence the reaction rates of the biochemical pathways involved in sulfate reduction. Based on observed fractionation patterns and the fractionation model developed by Rees (1973), isotope fractionation should be minimized if sulfate transport into the cell is rate limiting because fractionations associated with the different reduction steps (steps 3 and 4, Eq. (7)) will not be expressed. Conversely, fractionation will be maximized when exchange between the reversible steps in the sulfate reduction process is maximized. In most isotope fractionation models, this is best achieved when the microbial metabolism is suppressed. We explored how changes in hydrogen availability and temperature affected fractionation by the thermophilic and chemolithoautotrophic *T. indicus*. The results showed that sulfate reduction rates and the extent of fractionation were sensitive to both hydrogen availability and temperature (Figs. 1 and 3).

The reduced fractionations typically observed when H_2 is used as a non-limiting electron donor is thought to result from the ready supply of electrons for the reduction of APS and sulfite, through the efficient operation of hydrogenase enzymes (Rees, 1973; Canfield, 2001a). This would minimize reverse enzymatic reactions, reducing isotope exchange. This interpretation is supported by experiments with *D. vulgaris* which showed generally higher sulfate

reduction rates when H_2 was used as the electron donor compared to growth with an organic electron donor under similar conditions (Kaplan and Rittenberg, 1964; Kemp and Thode, 1968). In the fed-batch experiments with reduced H_2 supply specific growth rates dropped ~50-fold compared to growth rates under non-limited H_2 conditions. This corresponded to a significant drop in sulfate reduction rates (Fig. 1). The dramatic increase in fractionation which occurred when H_2 supply to the reactor was restricted may be due to a decrease in the electron flux through hydrogenase pathways and points to the importance of the rate of electron supply in controlling fractionation. Limiting the rate of enzymatic reduction of APS and sulfite (steps 3 and 4, Eq. (7)), in turn facilitates isotope exchange between internal sulfate and sulfite and consequently between internal and external sulfate thereby maximizing fractionation (reviewed in Canfield, 2001a).

It is generally observed that fractionations are reduced at the lower and higher ends of a growth temperature range (e.g., Kaplan and Rittenberg, 1964; Canfield, 2001b). At lower temperatures this is attributed to a reduction of the fluidity of the cell membrane, reducing sulfate exchange across the membrane. At higher temperatures, accelerating sulfate reduction rates increase sulfate demand by the cell effectively reducing sulfate exchange across the cell membrane. Although observations of fractionation by pure cultures and natural populations support this model (e.g., Harrison and Thode, 1958; Kaplan and Rittenberg, 1964; Brüchert et al., 2001; Canfield, 2001b), some pyschrophilic strains show little temperature effect on fractionation (Brüchert et al., 2001). Our results however, show trends with temperature and sulfate reduction rates (Fig. 3) that differ from most previously observed. We obtained the lowest fractionations at 60 °C, which is below the optimal growth temperature and above the lowest temperature for growth, with fractionations increasing away from this temperature (Fig. 3). Kaplan and Rittenberg (1964) and Kemp and Thode (1968) in a much more limited way explored how temperature influenced fractionation of resting suspensions of different *Desulfovibrio* strains with H_2 as the electron donor. They report that fractionations increased with increasing sulfate reduction rates, which generally increased with increasing temperatures. Although these results are consistent with our observations between 60 and 70 °C, they are inconsistent with our observations at other temperatures (Fig. 3). While some of these differences may be attributed to strain-specific differences in the controls of fractionation, the discrepancy between our results and those of Kaplan and Rittenberg (1964) and Kemp and Thode (1968), may partially result from the broader growth-temperature range covered in our experiments. Interestingly, similar temperature-dependant fractionation trends were also observed by Canfield et al. (2006) for the mesophilic sulfate-reducing bacterium *Desulfovibrio desulfuricans*. Both our results, and those of Canfield et al. (2006), show consistent patterns that are not consistent with most previous observations and discussions on the control of temperature on fractionation.

The switch in the fractionation trends observed at 60 °C may, in part, result from a transition in the fluidity of the cell membrane from a rigid gel-like structure to a more fluid liquid-crystalline structure (Singer and Nicolson, 1972). Rapid transitions in membrane fluidity occur in most organisms with a lipid bi-layer at temperatures just below the optimal growth temperature for the organism. The temperature at which the phase transition of the cell membrane occurs is specific to each organism and reflects the lipid composition of the cell membrane for an organism. Temperature-dependent membrane structural transitions can have dramatic effects on the activity of intrinsic membrane proteins such as membrane-transport proteins.

In general, our fractionation results indicate that different environmental factors such as temperature and substrate availability have a significant impact on different parts of the sulfate reduction process, and conversely that different pathways of the sulfate reduction process respond differently to environmental factors.

4.3. Isotope fractionation model

Canfield et al. (2006) have used the 'standard' model of Rees (1973) to explain all observed fractionation patterns by developing a quantitative framework against which specific fractionation trends can be tested. The model builds on the reaction network for sulfate reduction originally developed by Rees (1973), and formalized by Farquhar et al. (2003)

$$SO_{4\,(out)}^{=} \underset{2,\varphi 2,\alpha 2}{\overset{1,\varphi 1,\alpha 1}{\rightleftarrows}} \left[SO_{4\,(in)}^{=} \underset{5a}{\overset{4a}{\rightleftarrows}} APS \underset{5b,\varphi 5,\alpha 5}{\overset{4b,\varphi 4,\alpha 4}{\rightleftarrows}} SO_3^{=} \right] \overset{3,\varphi 3,\alpha 3}{\rightarrow} H_2S \qquad (8)$$

The numbers designate different steps, φ represents mass flow, and α is the fractionation factor associated with each step. In this model, Canfield et al. (2006) use the same fractionation values as those used by Rees (1973) (see Section 4.1). Branching points within the network control mass balance where material flow has two possible paths. The first branching point is defined for the transport of sulfate across the cell membrane and a second branching point is defined for the extent to which sulfite formation is reversible. Canfield et al. (2006) present equalities that describe the controls on mass flow at each branch point. With the first branch point, the fraction of sulfur exiting the cell as sulfide compared to the total amount of sulfur entering the cell is given by

$$f_3 = \frac{\varphi_3}{\varphi_2 + \varphi_3}. \qquad (9)$$

In the second branch point, the fraction of sulfite that is further reduced to sulfide is given by

$$f_5 = \frac{\varphi_3}{\varphi_5 + \varphi_3}. \qquad (10)$$

From these equalities and isotope mass balance, the following expressions describe the influence of f_3 and f_5 on the isotopic composition of sulfide generated from sulfate reduction. The first expression:[1]

$$rSO_{4(in)} = \frac{rH_2S + rH_2S^2 - f_5 rH_2S + \alpha_3 f_5 rH_2S}{\alpha_5[\alpha_3 + \alpha_3 rH_2S + f_5 rH_2S - \alpha_3 f_5 rH_2S]} \quad (11)$$

describes the isotopic composition of internal sulfate where r represents the isotope ratio ($^{34}S/^{32}S$) for a particular species. The second expression relates the isotopic composition of sulfate outside the cell to the isotopic composition of internal sulfate:

$$rSO_{4(out)} = \frac{rSO_{4(in)} + rSO_{4(in)} rH_2S - f_3 rSO_{4(in)} + f_3 rH_2S}{\alpha_1\left[1 + rH_2S + f_3 rSO_{4(in)} - f_3 rH_2S\right]}. \quad (12)$$

To analyze the relationship between f_3, f_5, and the fractionation of sulfide, we first fix values for f_3 and f_5, and then choose rH_2S to return values of $rSO_{4(in)}$ (Eq. (11)). These values are then used to recover the given value for $rSO_{4(out)}$ (Eq. (12)). This model predicts that changes in mass flow of either sulfate exchange in and out of the cell, f_3, or the exchange of internal sulfate with sulfite, f_5, will significantly affect the fractionation. Maximum possible fractionations are expressed when both f_5, and f_3 are small (i.e., when the exchange of sulfate across the membrane and exchange of internal sulfur pools are maximized). It is important to recognize that a particular pair of f_3, and f_5 is not necessarily unique for a given value of $\delta^{34}S_{H_2S}$ (Fig. 4) and any results obtained from this model are only best estimates as to how the combined effects of f_3, f_5, and internal fractionations control the final expression of isotope fractionation. There is however, only a single correct f_3, f_5 pair each at either fractionation extreme (−3‰ and 47‰, $\varepsilon_{SO_4(out)-H_2S}$), and as fractionation values move away from either extreme, the number of possible f_3, f_5 pairs for a given fractionation value increase (Fig. 4). In general, for a given fractionation value there is a much greater range of possible f_5 values than f_3 values (especially for f_3 values between 0.5 and 1). This implies that the exchange of sulfate in and out of the cell varies less, and exerts a greater influence on the extent of fractionation than the exchange of internal sulfur reservoirs below fractionations of about 20‰ ($\varepsilon_{SO_4(out)-H_2S}$) (Fig. 4). Importantly, Canfield et al. (2006) note that with these expressions unique solutions for f_3 and f_5 can be determined if the isotopic composition of the internal sulfate pool and all of the internal fractionations (α values) are known.

Within the framework of this model, we can re-create the fractionation trends observed in our experiments by exploring how different values of f_3 and f_5 reproduce the measured fractionations. Thus, in the fed-batch experiments where hydrogen availability was limited, the high fractionation values (37‰) were reproduced when both f_3 and f_5 are low (Table 2 and Fig. 4). The low possible values of both f_3 (0–0.2) and f_5 (0–0.4) indicate that the internal sulfate pool exchanges readily with external sulfate under these conditions, and that the mass flow of sulfite to APS (step 5b, Eq. (8)), and possibly APS to $SO^{2-}_{4\ (in)}$ (step 5, Eq. (8)) is large. A likely interpretation of this scenario is that under these conditions the reduced rate of supply of electrons from H_2 limits the reduction rate of both APS and sulfite and suggests that the reduction of sulfite (step 3, Eq. (8)) rather than the exchange of sulfate across the cell membrane (steps 1 and 2, Eq. (8)) becomes rate limiting.

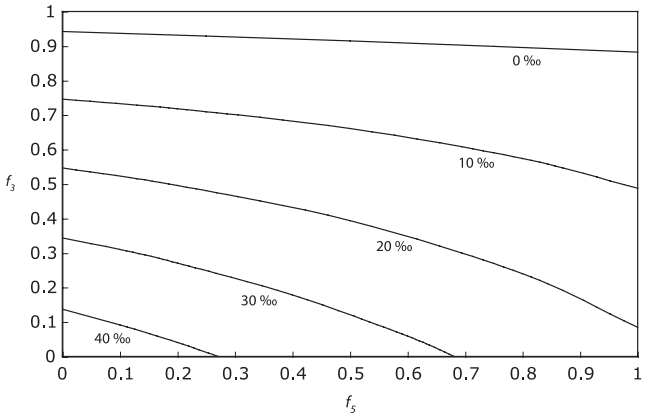

Fig. 4. Plot showing the range of possible f_3 and f_5 values for given fractionation values. Selected $\varepsilon_{(SO_4(out)-H_2S)}$ values of each line are shown on the plot. There is only a single possible f_3, f_5 pair for the extreme fractionation values of −3‰ (f_3, $f_5 = 1{,}0$) and 47‰ (f_3, $f_5 = 0{,}0$).

Under sustained conditions of excess hydrogen at optimal growth temperatures (70 °C) in the bioreactor, possible values of f_3 (0.8–0.9) and f_5 (0–1.0) show that f_3 values do not vary much with respect to f_5 values. Fractionation values (3.5–4‰, $\varepsilon_{SO_4(out)-H_2S}$) were similar to the values obtained for batch cultures in the heat-block experiments growing around 70 °C (Figs. 1 and 3). Under these experimental conditions, it is expected that a high rate of sulfite reduction to sulfide (high f_5 values) reduces the mass flow of sulfite to APS (step 5b, Eq. (8)), and APS to $SO^{2}_{4(in)}$ (step 5, Eq. (8)), which minimizes isotope exchange between internal sulfur pools, and consequently between internal and external sulfate. These scenarios however, are not the only possible interpretations of how H_2-supply affects fractionation. Another possible interpretation is that H_2-sup-

Table 2
Values of f_3 and f_5 to reproduce experimental results of H_2-dependant fractionation experiments

H_2 flux	f_3	f_5	Fractionation
Low	0–0.2	0–0.4	37.8
High	0.8–0.9	0–1.0	3.5

[1] The expression for $rSO_{4(in)}$ reported by Canfield et al. (2006) was incorrectly printed. The exponent from the rH_2S^2 term was unintentionally omitted.

ply directly affects the rate of exchange of sulfate across the cell membrane through some unknown mechanism, rather than influencing the reduction rate of internal sulfate and sulfite. Thus, under conditions of high H_2-flux, exchange of sulfate across the cell membrane is somehow reduced, producing high f_3 values and leaving a wide range of possible f_5 values. This is unlikely to be the case however, because given our current understanding of the biochemistry of sulfate reduction there is no clear mechanism by which H_2 could directly influence the exchange of sulfate.

In the temperature-dependant experiments the range of observed fractionations could be reproduced by a range of f_3 and f_5 values (Table 3). As in the high H_2-flux experiments, f_3 values did not change very much across the range of observed fractionations, while f_5 values were completely unconstrained. Thus, the range of values of f_3 and f_5 that could reproduce the observed fractionations suggest that exchange of sulfate across the cell membrane is generally rate-limiting, and that the extent of fractionation is more sensitive to changes in the rate of sulfate exchange across the cell membrane (f_3) than the exchange of internal sulfur pools (f_5). The observed trends in fractionation with temperature could be reproduced by selecting specific values of f_3 and f_5 as they are predicted to respond to changes in temperature (Table 3). For example, as temperatures increase in the range from 45 to 60 °C, reduction rates of sulfite to sulfide also increase, and is likely to reduce exchange of the internal sulfate pool with sulfite. This would result in an increase in f_5 relative to f_3 and fractionations would decrease with increasing temperatures. In the temperature range from 60 to 70 °C, the rate of exchange of sulfate across the cell membrane may increase faster than the reduction rate of sulfite to sulfide generating a decrease in f_3 relative to f_5, and fractionations would increase with increasing temperatures.

Modeling of our experimental results predicts that rates of sulfate exchange across the cell membrane and reduction rates of sulfite to sulfide respond more strongly to temperature than the exchange between the internal sulfate pool and sulfite. The exchange between the internal sulfate pool and sulfite, however, is sensitive to changes in hydrogen availability.

4.4. Implications for sulfur isotope biosignatures at deep-sea vents and marine sediments

The large fractionations observed under hydrogen-restricted growth by *T. indicus* suggests that biogenic sulfide will be similarly depleted in ^{34}S under environmental conditions of deep-sea hydrothermal vents, where H_2 may be a growth-limiting substrate (Von Damm, 1995; McCollom and Shock, 1997; Tivey, 2004). Hydrogen concentrations in end-member hydrothermal fluid typically range from 0.05 to 1.5 mmol kg^{-1} and will decrease rapidly in the hydrothermal vent wall, due to increased seawater mixing, to concentrations in the low micromolar range (McCollom and Shock, 1997; Tivey, 2004). Although the exact H_2 concentration in the pore fluid of a chimney wall depends on several factors, including the structure and composition of the chimney wall, and the style of mixing between seawater and end-member vent fluid, we can approximate the concentration range of H_2 in a chimney wall at the temperature range for which *T. indicus* can grow (40–70 °C). If we assume a simplified model with batch-mixing of seawater and vent fluid across a one-layer wall, H_2 concentrations would range from 0.005 to 0.015 mmol kg^{-1} at 40 °C and 0.01–0.3 mmol kg^{-1} at 70 °C for the given range of typical H_2 concentrations in end-member vent fluid (0.05–1.5 mmol kg^{-1}). Although H_2 concentrations are not necessarily limiting under all expected conditions in the chimney, it is likely that H_2 concentrations are limiting bacterial hydrogenase activity in some parts of the chimney structure (Sonne-Hansen et al., 1999). Therefore, biogenic sulfide preserved as metal sulfides at deep-sea hydrothermal vents could also be depleted in ^{34}S by at least 24–37‰ with respect to seawater sulfate ($\delta^{34}S = 21‰$). Metal sulfides at deep-sea hydrothermal vents typically have $\delta^{34}S$ values ranging from 0‰ to 10‰ (Shanks, 2001), suggesting that biogenic sulfides formed in hydrothermal-vent sulfide deposits may be isotopically distinct from sulfides that have been abiotically produced under H_2-limited conditions. Conversely, H_2 may not be limiting in all deep-sea vent environments suggesting that apparent abiotic $\delta^{34}S$ values of sulfides may be indistinguishable from some of the measured values in this study under non-limiting H_2 conditions. In modern marine sediments, H_2 is typically maintained in the nano-molar range due to the activity of H_2-utilizing microorganisms such as sulfate reducers (Hoehler et al., 1998). These levels are much lower than is normally found in deep-sea vents environments and at these concentrations, mesophilic H_2-utilizing sulfate reducers in modern marine sediments are likely to be H_2-limited and would therefore generate biogenic sulfides significantly depleted in ^{34}S compared to seawater sulfate.

Because *T. indicus* is a deeply branching thermophilic chemolithoautotrophic bacterium isolated from a deep-sea hydrothermal vent, it may represent an appropriate analog for sulfate-reducing microorganisms that could have been active in hydrothermal systems of early Earth environments. The large fractionations measured under conditions of reduced H_2 supply suggest that biogenically formed sulfide minerals in ancient hydrothermal deposits may be similarly depleted in ^{34}S. However, because the extent of fractionation is dependant on multiple environmental factors, which include temperature, electron donor type

Table 3
The range of f_3 and f_5 that can reproduce experimental results of temperature dependant fractionation experiments

Temperature	f_3	f_5	Fractionation
Low	0.82–0.65 (0.8)	0–1 (0.1)	6.8
Medium	0.88–0.77 (0.8)	0–1 (0.7)	3.8
High	0.75–0.5 (0.6)	0–1 (0.7)	10.2

and concentration, and sulfate concentration, it may be difficult to identify biogenic isotopic signatures in ancient hydrothermal deposits. This would be particularly true in ancient hydrothermal deposits of Archaean age where an ocean with low (<200 μM) sulfate concentrations may have existed (Canfield et al., 2000; Habicht et al., 2002).

5. Conclusions

In this study we have examined the fractionation of sulfur isotopes by *T. indicus*, a thermophilic chemolithoautotrophic sulfate-reducing bacterium that was recently isolated from a deep-sea hydrothermal vent on the Central Indian Ridge (Moussard et al., 2004). We measured changes in sulfur-isotope fractionation over a wide range of temperatures, as well as under saturated and reduced hydrogen flux. This is the first report of the effect on fractionation of conditions where hydrogen is a limiting substrate.

High fractionations approaching 40‰ were obtained when *T. indicus* was grown under conditions of reduced hydrogen supply compared to fractionations (~3‰ and 5‰) obtained under conditions of excess hydrogen. Such high fractionations have never been reported with growth on hydrogen. This large difference in fractionation paralleled a large change in sulfate-reduction rates. It is likely that the reduced hydrogen flux through the reactor resulted in lower hydrogenase activity, which slowed sulfate reduction rates and allowed isotope exchange of internal sulfur pools. This would cause an increased expression of the fractionation factors of individual enzymatic reduction steps during sulfate reduction. The model from Canfield et al. (2006) was able to reproduce the large fractionations observed under low hydrogen flux when both the sulfate exchange out of the cell, and isotopic exchange between the internal sulfur pools was maximized (f_3 and $f_5 \Rightarrow 0$).

Specific sulfate-reduction rates increased with increasing temperatures, reaching maximum values at 70 °C. Variations of growth temperature yielded fractionations ranging from ~3‰ to 10‰ over a temperature range of 45–80 °C. Fractionations decreased with increasing sulfate-reduction rates in the temperature range from 45 to 60 °C, and increased with increasing sulfate-reduction rates from 60 to 70 °C. Above 70 °C fractionations were more variable but generally increased with increasing sulfate reduction rates. These temperature dependant trends in fractionation are different from what has generally been observed, and from what is predicted by a standard fractionation model. Our results and those predicted by the 'standard model' can be explained by the fractionation model of Canfield et al. (2006), that considers the mass flow of sulfur through different steps in the sulfate reduction pathway. The modeling results suggest that changes in fractionation are controlled by the extent to which (1) sulfate exchanges in and out of the cell and (2) the extent to which sulfur exchanges between the internal sulfur pools.

Acknowledgments

We thank Peter Søholt and Lilian Salling and members of the J.J.L. Iversen lab for expert technical and analytical assistance. We thank Poul Esbensen and Bent Bach Andersen for help in construction of the gradient temperature block. We thank C. Jeanthon for providing cultures of *T. indicus*. We also thank K. Mandernack, S. Bernasconi, and two anonymous reviewers for critical reviews of this manuscript. This research was supported by a NASA-Exobiology Grant (NAG5-13503), the Danish National Research Foundation (Danmarks Grundforskningsfond), and the International School of Aquatic Sciences (SOAS).

Associate editor: Timothy W. Lyons

References

Bolliger, C., Schroth, M.H., Bernasconi, S.M., Kleikemper, J., Zeyer, J., 2001. Sulfur isotope fractionation during microbial sulfate reduction by toluene-degrading bacteria. *Geochim. Cosmochim. Acta* **65**, 3289–3298.

Bottcher, M.E., Sievert, S.M., Kuever, J., 1999. Fractionation of sulfur isotopes during dissimilatory reduction of sulfate by a thermophilic gram-negative bacterium at 60 °C. *Arch. Microbiol.* **172**, 125–128.

Brüchert, V., Knoblauch, C., Jorgensen, B.B., 2001. Controls on stable sulfur isotope fractionation during bacterial sulfate reduction in Arctic sediments. *Geochim. Cosmochim. Acta* **65**, 763–776.

Brunner, B., Bernasconi, S.M., 2005. A revised isotope fractionation model for dissimilatory sulfate reduction in sulfate reducing bacteria. *Geochim. Cosmochim. Acta* **69**, 4759–4771.

Canfield, D.E., 2001a. Biogeochemistry of sulfur isotopes. In: *Stable Isotope Geochemistry*. In: Valley, J.W., Cole, D.R. (Eds.), *Reviews in Mineralogy and Geochemistry*, vol. 43. Mineralogical Society of America, USA, pp. 607–636.

Canfield, D.E., 2001b. Isotope fractionation by natural populations of sulfate-reducing bacteria. *Geochim. Cosmochim. Acta* **65**, 1117–1124.

Canfield, D.E., Habicht, K.S., Thamdrup, B., 2000. The Archean sulfur cycle and the early history of atmospheric oxygen. *Science* **288**, 658–661.

Canfield, D.E., Teske, A., 1996. Late Proterozoic rise in atmospheric oxygen concentration inferred from phylogenetic and sulphur-isotope studies. *Nature* **382**, 127–132.

Canfield, D.E., Thamdrup, B., Kristensen, E., (2005). Aquatic Geomicrobiology. *Advances in Marine Biology 48*. San Diego, CA, Academic Press, pp. 656.

Canfield, D.E., Olesen, C.A., Cox, R.P., 2006. Temperature, sulfate exchange, and isotope fractionation by a sulfate-reducing bacterium. *Geochim. Cosmochim. Acta.* **70**, 548–561.

Chambers, L.A., Trudinger, P.A., Smith, J.W., Burns, M.S., 1975. Fractionation of sulfur isotopes by continuous cultures of Desulfovibrio desulfuricans. *Can. J. Microbiol.* **21**, 1602–1607.

Cline, J.D., 1969. Spectrophotometric determination of hydrogen sulfide in natural waters. *Limnol. Oceanogr.* **14**, 454–458.

Cypionka, H., 1995. Solute transport and cell energetics. In: Barton, L.L. (Ed.), *Sulfate-Reducing Bacteria*. Plenum Press, New York, pp. 151–184.

Dahl, C., Trüper, H.G., 1994. Enzymes of dissimilatory sulfide oxidation in phototrophic sulfur bacteria. In: *Methods in Enzymology. Inorganic Microbial Sulfur Metabolism*. In: Peck, H.D., JrJr, LeGall, J. (Eds.), *Methods in Enzymology*, vol. 243. Academic Press, New York, pp. 400–421.

Detmers, J., Bruchert, V., Habicht, K.S., Kuever, J., 2001. Diversity of sulfur isotope fractionations by sulfate-reducing prokaryotes. *Appl. Environ. Microbiol.* **67**, 888–894.

Elsgaard, L., Isaksen, M.F., Jorgensen, B.B., Alayse, A.M., Jannasch, H.W., 1994. Microbial sulfate reduction in deep-sea sediments at the Guaymas Basin—Hydrothermal Vent Area—influence of temperature and substrates. *Geochim. Cosmochim. Acta* **58**, 3335–3343.

Farquhar, J., Johnston, D.T., Wing, B.W., Habicht, K.S., Canfield, D.E., Airieau, S., Thiemens, M.H., 2003. Multiple sulphur isotopic interpretations of biosynthetic pathways: implications for biological signatures in the sulphur isotope record. *Geobiology* **1**, 27–36.

Giesemann, A., Jager, H.J., Norman, A.L., Krouse, H.P., Brand, W.A., 1994. Online sulfur-isotope determination using an elemental analyzer coupled to a mass-spectrometer. *Anal. Chem.* **66**, 2816–2819.

Habicht, K.S., Gade, M., Thamdrup, B., Berg, P., Canfield, D.E., 2002. Calibration of sulfate levels in the Archean Ocean. *Science* **298**, 2372–2374.

Habicht, K.S., Salling, L.L., Thamdrup, B., Canfield, D.E., 2005. Effect of low sulfate concentrations on lactate oxidation and isotope fractionation during sulfate reduction by Archaeoglobus fulgidus strain Z. *Appl. Environ. Microbiol.* **71**, 3770–3777.

Harrison, A.G., Thode, H.G., 1957. The kinetic isotope effect in the chemical reduction of sulphate. *Trans. Faraday Soc.* **53**, 1648–1651.

Harrison, A.G., Thode, H.G., 1958. Mechanism of the bacterial reduction of sulphate from isotope fractionation studies. *Trans. Faraday Soc.* **54**, 84–92.

Hoehler, T.M., Alperin, M.J., Albert, D.B., Martens, C.S., 1998. Thermodynamic control on hydrogen concentrations in anoxic sediments. *Geochim. Cosmochim. Acta* **62**, 1745–1756.

Hoek, J., Canfield, D.E., Reysenbach, A.L., Iversen, J.J.L., 2006. A bioreactor for growth of sulfate-reducing bacteria: Online estimation of specific growth rate and biomass for the deep-sea hydrothermal vent thermophile Thermodesulfatator indicus. *Micro. Ecol.* **51**, 470–478.

Johnston, D.T., Farquhar, J., Wing, B.W., Kaufman, A.J., Canfield, D.E., Habicht, K.S., 2005. Multiple sulfur isotope fractionations in biological systems. *Am. J. Sci.* **305**, 645–660.

Kaplan, I.R., Rittenberg, S.C., 1964. Microbiological fractionation of sulphur isotopes. *J. Gen. Microbiol.* **34**, 195–212.

Kemp, A.L.W., Thode, H.G., 1968. Mechanism of bacterial reduction of sulphate and of sulphite from isotope fractionation studies. *Geochim. Cosmochim. Acta* **32**, 71–91.

Kleikemper, J., Schroth, M.H., Bernasconi, S.M., Brunner, B., Zeyer, J., 2004. Sulfur isotope fractionation during growth of sulfate-reducing bacteria on various carbon sources. *Geochim. Cosmochim. Acta* **68**, 4891–4904.

McCollom, T.M., Shock, E.L., 1997. Geochemical constraints on chemolithoautotrophic metabolism by microorganisms in seafloor hydrothermal systems. *Geochim. Cosmochim. Acta* **61**, 4375–4391.

McCready, R.G.L., 1975. Sulfur isotope fractionation by Desulfovibrio and Desulfotomaculum species. *Geochim. Cosmochim. Acta* **39**, 1395–1401.

Moussard, H., L'Haridon, S., Tindall, B.J., Banta, A., Schumann, P., Stackebrandt, E., Reysenbach, A.L., Jeanthon, C., 2004. Thermodesulfatator indicus gen. nov., sp. nov., a novel thermophilic chemolithoautotrophic sulfate-reducing bacterium isolated from the Central Indian Ridge. *Int. J. Syst. Evol. Microbiol.* **54**, 227–233.

Peck, H.D., 1961. Evidence for reversibility of reaction catalyzed by adenosine 5′-phosphosulfate reductase. *Biochim. Biophys. Acta* **49**, 621.

Porter, K.G., Feig, Y.S., 1980. The use of DAPI for identifying and counting aquatic microflora. *Limnol. Oceanogr.* **25**, 943–948.

Rees, C.E., 1973. A steady state model for sulphur isotope fractionation in bacterial reduction processes. *Geochim. Cosmochim. Acta* **37**, 1141–1162.

Shanks, W.C.I., 2001. Stable isotopes in seafloor hydrothermal systems: vent fluids, hydrothermal deposits, hydrothermal alteration, and microbial processes. In: *Stable Isotope Geochemistry*. In: Valley, J.W., Cole, D.R. (Eds.), *Reviews in Mineralogy and Geochemistry*, vol. 43. Mineralogical Society of America, USA, pp. 469–525.

Singer, S.J., Nicolson, G.L., 1972. Fluid mosaic model of the structure of cell-membranes. *Science* **175**, 720–731.

Smejkal, V., Cook, F.D., Krouse, H.R., 1971. Studies of sulfur and carbon isotope fractionation with microorganisms isolated from springs of Western Canada. *Geochim. Cosmochim. Acta* **35**, 787–800.

Sonne-Hansen, J., Westermann, P., Ahring, B.K., 1999. Kinetics of sulfate and hydrogen uptake by the thermophilic sulfate-reducing bacteria Thermodesulfobacterium sp. strain JSP and *Thermodesulfovibrio* sp. strain R1Ha3. *Appl. Environ. Microbiol.* **65**, 1304–1307.

Thode, H.G., Kleerekoper, H., McElcheran, D.E., 1951. Sulphur isotope fractionation in the bacterial reduction of sulphate. *Res. London* **4**, 581–582.

Tivey, M.K. (2004). Environmental conditions within active seafloor vent structures: sensitivity to vent fluid composition and fluid flow. In: Wilcock, W., Cary, C., DeLong, E., Kelley, D., Baross, J. (Eds.), *Subseafloor Biosphere at Mid-Ocean Ridges*. Geophysical Monograph, American Geophysical Union.

Von Damm, K.L., 1995. Controls on the chemistry and temporal variability of seafloor hydrothermal fluids. In: Humphris, S.E., Zierenberg, R.A., Mullineaux, L.S., Thomson, R.E. (Eds.), *Seafloor hydrothermal systems: physical, chemical, biological, and geological interactions*. American Geophysical Union, pp. 222–247.